🔓 OPEN ACCESS

A Long Short-Term Memory Network for Product Quality Monitoring in Fused Deposition Modeling

Md Emon Ahmed[1], Nur Mohammad Ali[2], Mohammad Shah Paran[3], Abdur Rahman[3], Jayanta Bhusan Deb[4*]

[1]Zicklin School of Business, Bernard M. Baruch College, City University of New York, NY, USA
[2]Department of Industrial Engineering, Lamar University, TX, USA
[3]Department of Electrical Engineering, Lamar University, TX, USA
[4]Department of Mechanical and Aerospace Engineering, University of Central Florida, FL, USA

Abstract		Original Research Article

This study investigated the influence of room temperature on the final prototype parts produced using the fused deposition modeling (FDM) technique. Real-time room temperature data was collected using a wireless sensor with a time series data collection method. A data-driven model called Long Short-Term Memory (LSTM) network was developed to predict room temperature. The model was trained using data from the wireless sensors collected during the experimental procedure, which involved printing prototype parts in different seasons of the year. The developed LSTM network demonstrated its capability to accurately predict temperature, enabling the detection of printing defects under various room temperature conditions. The study revealed that lower room temperatures had a more significant impact on the surface roughness of the printed parts compared to higher room temperatures. The effectiveness of the developed model was confirmed by comparing its results with the experimental data using Root Mean Square Error (RMSE). The developed LSTM model found an RMSE of 0.003993 for predicting cold room temperature data and an RMSE of 0.033993 for predicting hot temperature data. The developed LSTM model offers a valuable tool for detecting printing defects in different room temperature conditions. It provides users with information about the room temperature necessary for printing high-quality parts, thereby enhancing the printing process capability and minimizing defect issues in the printed parts.

Keywords: Additive manufacturing; Fused deposition modeling; Long short-term memory; Temperature prediction; Real-time product quality monitoring.

1. INTRODUCTION

Additive manufacturing (AM), or 3D printing, is a cutting-edge technique to create three-dimensional objects based on computer-aided design (CAD) models. This technology has gained significant attention and popularity across various industries, including automotive, aerospace, construction, medicine, and architecture [1,2]. One of the key advantages of 3D printing is its ability to produce complex structures that would be challenging to achieve using traditional manufacturing methods [3]. The flexibility of 3D printing allows the creation of unique shapes, geometries, and customized products tailored to specific requirements [4]. Another advantage of 3D printing is its efficiency and cost-effectiveness [5]. Unlike traditional manufacturing processes, which often involve multiple stages such as casting, molding, milling, and cutting 3D printing is a single-stage process [6]. This eliminates the need for tooling and reduces material waste, resulting in cost savings and improved production efficiency [7]. Furthermore, 3D printing offers greater design freedom and customization options. It allows designers and engineers to quickly iterate and modify designs, making incorporating design improvements and responding to customer needs easier [8]. This flexibility is particularly beneficial in industries where customized products are required.

Fused Deposition Modeling (FDM), also referred to as Fused Filament Fabrication (FFF), is a widely used 3D printing technique that involves the extrusion of thermoplastic material to create three-dimensional objects [9]. This method has gained popularity, particularly in fields such as aerospace and medical science, due to its simplicity in post-processing, a wide range of material options, and cost-effectiveness

compared to other additive manufacturing methods [10]. While FDM offers several advantages, achieving high-quality printed parts can be challenging due to various factors. These factors include process parameters and the manufacturing environment where the printing takes place. The selection and optimization of these parameters are crucial in ensuring the desired quality and performance of the printed objects [11]. Process parameters in FDM, such as layer thickness, nozzle temperature, printing speed, build orientation, and deposition direction, directly influence the outcome of the printing process. The layer thickness affects the resolution and surface finish of the printed part [5], while the nozzle temperature determines the material's melting and extrusion properties [12]. Printing speed and build orientation impact the final object's printing time and mechanical properties [13]. Therefore, it is essential to carefully select and optimize these parameters based on the specific requirements of the printed parts. Additionally, the manufacturing environment can also impact the quality of FDM-printed parts. Room temperature, humidity, and air circulation can influence the material's cooling rate, warping, and overall dimensional accuracy of the FDM printed parts [11]. These variables can also impact the printed parts' geometry, mechanical strength, surface quality, and process stability [11]. So, it is essential to establish a reliable quality monitoring system for analyzing the impact of environmental factors on part quality and to ensure a consistent AM process with desirable quality outcomes [14]. Therefore, controlling and maintaining a stable and suitable room temperature environment is crucial for achieving consistent and reliable printing results, as it is very difficult to control the room temperature during 3D printing process in the third world country like Bangladesh.

In this study, we developed a Long Short-Term Memory (LSTM) network to detect anomalies in the printing process based on fluctuations in room temperature. The significant contribution of our research lies in the effectiveness of our LSTM model in identifying product defects at different times of the day, utilizing room temperature data. This model can assist users in the early defect detection of product defects during the printing process and make informed decisions about whether to proceed with printing based on the room temperature conditions for that day. The remaining sections of this research paper are structured as follows: Section 2 covers a thorough literature assessment of various sensors utilized in FDM for online monitoring as well as pertinent machine learning techniques applied to FDM to forecast the quality of final products. The specimen, materials, and machine learning model used in this study are introduced in Section 3, along with the experiment design and created time series data collection experimental and simulation method. Results from experiments and simulations are presented in Section 4. Section 5 offers a conclusion and suggestions for future development.

2. LITERATURE REVIEW
To ensure the printed parts meet the desired specifications, extensive research, and experimentation are conducted to identify the optimal process parameters and environmental conditions for each specific application [15]. This optimization process involves iterative testing, adjustments, and validation to fine-tune the parameters [5, 16]. By optimizing the FDM process parameters and controlling the manufacturing environment, manufacturers can overcome the challenges associated with FDM printing and achieve high-quality, functional, and cost-effective 3D printed objects that meet various industries' specific requirements.

Machine Learning has emerged as a valuable tool in the manufacturing industry, particularly in monitoring and predicting the quality of printed components [17–20]. By leveraging images and processing data, machine learning algorithms can analyze and predict the expected quality of printed objects [21–23]. Cameras and sensors capture and monitor on-site process data [24]. These devices record various parameters and variables related to the printing process, such as temperature, humidity, material flow, nozzle movement, and other relevant factors. The collected data serves as input for the Machine Learning algorithms, enabling them to learn patterns, correlations, and anomalies in the manufacturing process [25]. Artificial intelligence-based process analyses and computer-based learning processes are then applied to evaluate the recorded data [26]. Machine Learning algorithms are trained on historical data, allowing them to identify patterns and trends that can be used to predict future data [27]. By continuously monitoring and analyzing the process data in real time, the algorithms can provide early conclusions and insights regarding the printing process and the expected quality of the printed components [28]. Furthermore, to validate the post-printing manufacturing results and evaluate the component quality, optical 3D scans are performed. These scans provide detailed information about the printed objects' geometry, dimensions, surface finish, and other relevant characteristics. By comparing the scanned data with the predicted results from the Machine Learning model, manufacturers can assess the accuracy and reliability of their predictions [11]. By combining data analysis, and machine learning algorithms, manufacturers can gain valuable insights into the printing process and the quality of the printed components. This enables them to detect potential issues or deviations early on, make informed decisions, and take corrective actions to ensure the production of high-quality and reliable printed objects.

Developing a real-time monitoring system for Fused Deposition Modeling (FDM) machine conditions is a crucial advancement in ensuring the quality and reliability of the printing process [29]. This system analyzes acoustic emission data to detect abnormal

conditions and potential errors during FDM printing. Acoustic emission data refers to the signals or vibrations generated by the FDM machine during operation [30]. These signals carry valuable information about the machine's performance and can be analyzed to identify patterns and characteristics associated with normal or abnormal system conditions. By monitoring and analyzing the acoustic emission data in real-time, the monitoring system can detect deviations from expected patterns that may indicate issues or errors in the printing process [31]. The real-time monitoring system employs a Support Vector Machine (SVM) algorithm to distinguish between normal and abnormal system conditions. SVM is a machine learning algorithm that excels in classification tasks by identifying decision boundaries between different categories based on labeled training data [32]. Therefore, the SVM algorithm is trained using acoustic emission data from known normal and abnormal system conditions. Once trained, the SVM algorithm can classify new acoustic emission data in real time and identify whether the FDM machine is operating normally or experiencing anomalies [33]. While CNN-based image recognition systems are also available for error detection in the FDM printing process, their capabilities are limited to identifying obvious geometry defects [24, 34]. These systems analyze the visual characteristics of the printed parts to detect visible flaws or irregularities that are readily apparent in the images [30]. However, they may be unable to detect certain errors or abnormalities that do not manifest as obvious visual defects.

Long Short-Term Memory (LSTM) networks are a commonly used machine learning technique for predicting time series sequential data [35–38]. To mitigate the risk of thermal degradation among manufactured products using an FDM machine, a shallow Long Short-Term Memory algorithm was used to forecast the thermal state of the extruder using data gathered from a temperature sensor during the normal printing process [12]. A new technology using multi-sensor data has been proposed to detect FDM printers' different working conditions. The technology used a classification LSTM network to distinguish among various working conditions of FDM printing based on the clamping force. To detect normal and faulty states of the printer, this method could be used over traditional single sensor monitoring to improve the accuracy of monitoring and identifying different working conditions. More information could be collected by using multiple sensors leading to significantly improved accuracy in detecting different working conditions of FDM equipment [39].

Previous studies primarily focused on real-time monitoring of the additive manufacturing process to detect faults in the FDM printer and assess the thermal performance of the extruder. However, little attention has been given to predicting how environmental factors affect the quality of the printed parts. We investigated a wireless sensor-based approach to monitor and analyze room temperature data to bridge this research gap.

3. METHODS
3.1 Modeling Specimen
The software Creo Parametric 6.0.4.0 was utilized to create the design for the ASTM D638-14 TYPE I sampled, as depicted in Fig 1 [40]. This had been done to ensure consistency with previous work in printing and measurement [39]. The resulting STL file was then sliced using the software PrusaSlicer Version 2.4.0+win64.
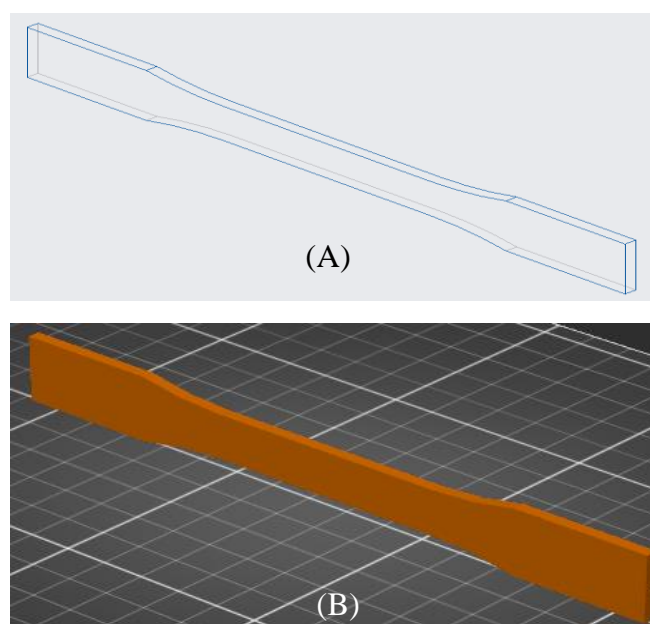
Fig 1: Design (A) and STL file (B) of the printed specimen at 90° build orientation

3.2 Materials, Printer, and AM Process Parameters Selection

In this research, PLA material was used for printing the specimen parts, a type of thermoplastic known for its environmental friendliness [5]. It was one of the most used 3D printing materials due to its ease of use, low cost, and availability. The 3D printing process was carried out using a Prusa i3 MK-3 3D printer, a widely used FDM 3D printer, and selected process parameters are shown in Table 1 [42]. We used constant process parameters for printing to check the effect of temperature in all parts. The constant process parameters were chosen after several trials to achieve maximum roughness in the surface. The process of depositing materials in alternating directions of 0° and 90° was done in a crisscross pattern as successive layers for all the parts, as shown in Fig 2.

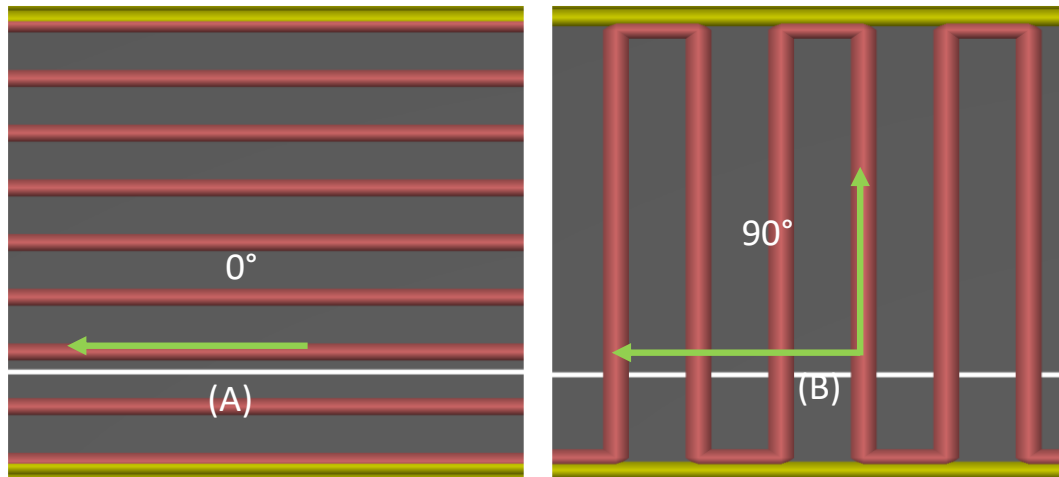**Fig 2: Infill angle (A) 0° and (B) 90° for rectilinear infill pattern [5]**

Table 1: Process parameters selection for printing specimen parts

Process Parameters	Value
Layer thickness	0.3 mm
Infill density	50%
Infill pattern	Rectilinear
Infill angle	0°
Extrusion speed	80 mm/s
Nozzle temperature	220°C
Build orientation	90°

3.3 Experimental Procedure

This study aimed to determine how the room's temperature impacted the final quality of the printed items. To achieve this goal, the experiment was conducted in a hot and cold room. The data on extremely cold room temperatures were gathered on February 1, 2023, during the winter in Cullowhee, North Carolina, USA, while the data on extremely hot room temperatures were gathered on July 23, 2022, during the summer at the same place. To precisely measure the room temperature, the heater in the winter and the air conditioner in the summer were switched off at the maker space at the Belk building of Western Carolina University. A wireless sensor called Wit Motion was used to measure the temperature, providing the time series data on room temperature.

Two prototype parts, in the shape of dog bones, were printed to examine the defects caused by extreme and cold room temperatures during the printing process. Each prototype took up to 1494 seconds to print, having 63 layers. A high-performance Lenovo laptop computer with a core i7 processor was utilized to collect real-time temperature data. The SPI Portable Roughness Tester II was used to measure the surface roughness of the printed parts to analyze the effect of temperatures on surface roughness. The Roughness tester used a stylus with a tip radius of .0002 inches to scan across the surface of the material to determine the surface roughness of the final parts.

3.4 Intelligence System Selection Process

The main goal of this study was to develop an optimal machine learning model for data-driven time series room temperature prediction in fused deposition modeling (FDM). A particular type of RNN known as Long Short-Term Memory (LSTM) was developed to solve the difficulties posed by long-term dependencies in recurrent neural networks (RNNs) [43]. A Lenovo laptop with an 11th Gen Intel(R) Core (TM) i7-11800H CPU and 16GB RAM was used to conduct the simulations and training of the LSTM model. These hardware specifications gave the model training process enough memory and processing capability. The Python module

Keras made implementing the LSTM model for predicting room temperature easier. It is an appropriate option for creating and optimizing the LSTM model in this study due to its simplicity.
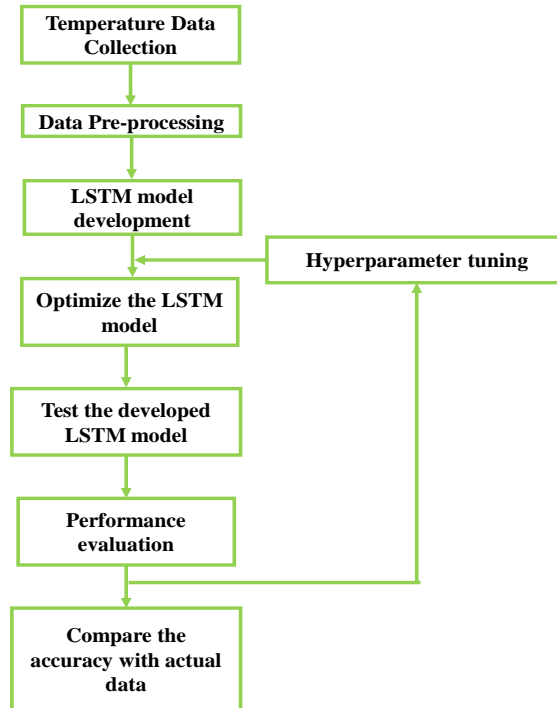
```
┌─────────────────────┐
│ Temperature Data    │
│ Collection          │
└─────────────────────┘
         │
┌─────────────────────┐
│ Data Pre-processing │
└─────────────────────┘
         │
┌─────────────────────┐
│ LSTM model          │
│ development         │
└─────────────────────┘
         │              ┌──────────────────────┐
         │◄─────────────│ Hyperparameter tuning│
┌─────────────────────┐ └──────────────────────┘
│ Optimize the LSTM   │            ▲
│ model               │            │
└─────────────────────┘            │
         │                         │
┌─────────────────────┐            │
│ Test the developed  │            │
│ LSTM model          │            │
└─────────────────────┘            │
         │                         │
┌─────────────────────┐            │
│ Performance         │            │
│ evaluation          │────────────┘
└─────────────────────┘
         │
┌─────────────────────┐
│ Compare the         │
│ accuracy with actual│
│ data                │
└─────────────────────┘
```

Fig 3: Intelligence system selection procedure

The various procedures involved in choosing the final LSTM model are shown in Fig 3. These procedures covered the many phases of model development, evaluation, and optimization. They covered activities including model data preprocessing, hyperparameter tuning, and performance assessment. The proposed framework is shown visually in Fig 4. These procedures act as a roadmap to guarantee a methodical and efficient model-building process, enabling researchers to make well-informed decisions and maximize the effectiveness of the LSTM model for room temperature prediction. The possibility of creating an optimal model that correctly forecasts future room temperature data in the context of FDM increases because of this methodical approach.
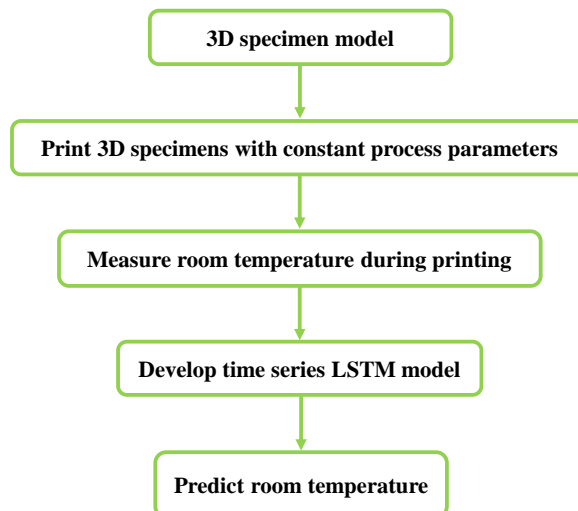
```
┌──────────────────────────────────────────┐
│            3D specimen model               │
└──────────────────────────────────────────┘
                     │
┌──────────────────────────────────────────┐
│ Print 3D specimens with constant process  │
│ parameters                                 │
└──────────────────────────────────────────┘
                     │
┌──────────────────────────────────────────┐
│ Measure room temperature during printing  │
└──────────────────────────────────────────┘
                     │
┌──────────────────────────────────────────┐
│ Develop time series LSTM model            │
└──────────────────────────────────────────┘
                     │
┌──────────────────────────────────────────┐
│ Predict room temperature                  │
└──────────────────────────────────────────┘
```

Fig 4: Proposed framework for LSTM modeling

3.5 LSTM Modeling

The LSTM approach emerged in 1997 to address the standard recurrent neural network's vanishing gradient issue [44]. A long short-term memory (LSTM) network that uses an input layer, one hidden layer of LSTM units, and an output layer to predict the future from sequential data is known as an LSTM network. The feedback connections in LSTMs set them apart from conventional feed-forward neural networks. With this feature, LSTM can handle a time series of data

as its whole rather than independently processing each data point. By proceeding this way, LSTM gathers essential data about prior data points in the series to forecast subsequent data sets. The LSTM model has thus been used to resolve challenging machine learning issues. LSTM networks with memory blocks are connected throughout the hidden layer in place of neurons. Memory blocks can update the data depending on the time series of sequential data. Because of this, memory blocks rather than neurons are used in LSTM's hidden layers [45].
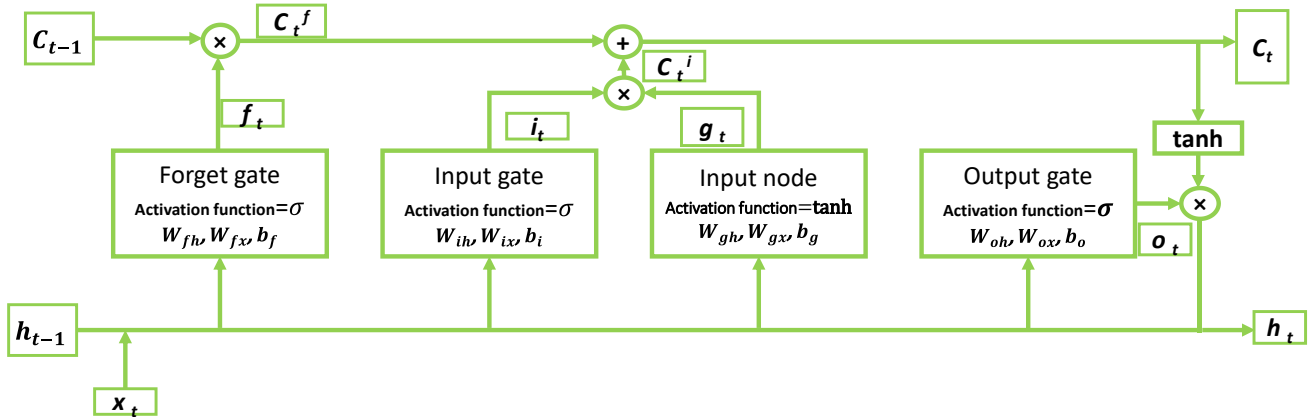
Fig 5: Forget, input and output gate in a cell of the LSTM network [46, 47]

The current cell state, the output of the previous hidden state, and the input data at the current time state all influence the LSTM network's output. A memory block in an LSTM network is made up of three gates: an output gate, an input gate, and a forget gate. Fig 5 depicts the network topology within a memory block. An input gate and an input node (new memory network) comprise the input gate. The forget gate determines which elements of the current data point and the prior hidden state in the sequence are given more or less weight. That is why it receives the previously hidden form and new input data; this network generates a vector in the range from 0 to 1 using the sigmoid activation function. Finally, the network in the forget gate receives the information when it is closer to 1 and vanishes the irrelevant information closer to 0. The goal of the input gate is to add new information to the network's long-term memory. After combining the previous hidden state and unknown input data, the input node generates a new memory update vector network with the help of $\tan h$ activation function, which contains the essential information. The input node is not capable of remembering new information. That is why the input gate comes up with a sigmoid activated, which works as a filter and makes the new memory update vector network worth retaining. So, the resulting information should be input gate regulated. After pointwise multiplication of the vectors generated from the input gate and input node (6), the resulting vector is added to cell state (5) to update the long-term memory of the network (7). The output gate uses updated cell state, previous hidden state, and new input data to generate a new hidden state. The output gate uses sigmoid activated neural network to store the relevant information. The output gate generates a filter vector from the previous hidden state and current input. Finally, pass the updated cell state to the $\tan h$ to force information to store between -1 to 1 [48]. Apply the filter vector to the updated cell. state as a pointwise multiplication to generate a new hidden state as output (8).

$$f_t = \sigma[(w_{fh}h_{t-1}) + (w_{fx}h_{t-1}) + b_f \ldots\ldots\ldots\ldots (1)$$
$$i_t = \sigma[(w_{ih}h_{t-1}) + (w_{ix}h_{t-1}) + b_i \ldots\ldots\ldots\ldots (2)$$
$$g_t = \tan h [(w_{gh}h_{t-1}) + (w_{gx}h_{t-1}) + b_g \ldots\ldots (3)$$
$$o_t = \sigma[(w_{oh}h_{t-1}) + (w_{ox}h_{t-1}) + b_o \ldots\ldots\ldots (4)$$
$$C_t^f = f_t C_{t-1} \ldots\ldots\ldots\ldots\ldots\ldots\ldots\ldots\ldots (5)$$
$$C_t^i = i_t g_t \ldots\ldots\ldots\ldots\ldots\ldots\ldots\ldots\ldots\ldots (6)$$
$$C_t = C_t^i + C_t^f \ldots\ldots\ldots\ldots\ldots\ldots\ldots\ldots\ldots (7)$$
$$h_t = \tan h (C_t)o_t \ldots\ldots\ldots\ldots\ldots\ldots\ldots\ldots (8)$$

Every gate inside a memory block is controlled by a sigmoid activation network but the input node used the $\tan h$ activation unit. Each block receives the previous hidden state and current data as input sequences. The result of forget gate, input gate, input node, and output gate are shown in (1)-(4) respectively. σ is a sigmoid and $\tan h$ is a tan activation function. w_{fh}, w_{ih}, w_{gh} and w_{oh} are the weights for hidden state and w_{fx}, w_{ix}, w_{gx} and w_{ox} are the weights for input of the respective gates, h_{t-1} is the output at time step ($t-1$) of the previous hidden state of LSTM block, b_f, b_i, b_g and b_o are biases for the respective gates and input is denoted by x_t at the current time step.

4. RESULTS DISCUSSION
4.1 LSTM Model Development Procedure
In our study, we concentrated on gathering time series data on room temperature under two different climates: cold and warm. The temperature information was an important consideration because it can have a impact on the quality of FDM produced parts. We developed a Long Short-Term Memory (LSTM) model to examine the connection between temperature and

printing results. Then, two sets—a training set and a testing set—of the gathered temperature data were created. The temperature measurements taken from the first forty-two layers of the FDM produced parts made up the training set, which made up 66.67% of the total temperature data. The remaining 33.33% of the data from layers forty-third to sixty-third made up the testing set.

1494 datapoints in total were gathered over the course of the experiment for the time series data. The first 996 of these datapoints were utilized to train the LSTM model, which helped it discover trends and connections between temperature and printing results. The remaining 498 data points were used to assess the model's performance and measure its precision as shown in Fig 6.
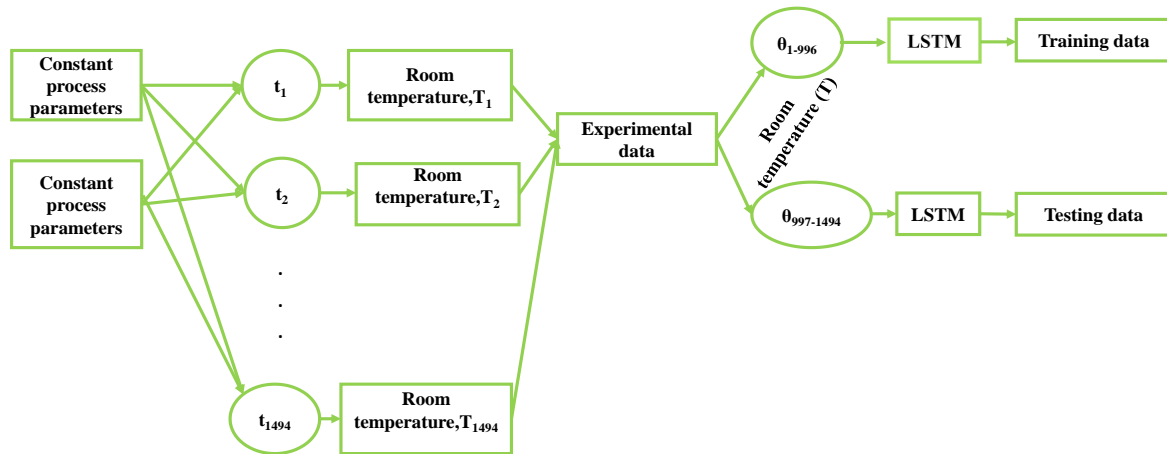
Fig 6: Sequential flow of training and testing data in the LSTM network

We tested the predicted temperature values against the actual temperature values in the testing dataset to see how accurately the LSTM model's predictions performed. The outcomes demonstrated that the model had good accuracy, especially over a lengthy training phase. This indicates that the LSTM model was successful in identifying the fundamental patterns and trends in the temperature data, which allowed it to produce accurate forecasts. Forecasting temperature variations and figuring out their effects on the printing results are made possible with the help of the LSTM model. To guarantee the best performance based on the available dataset, a neural network's hyperparameters must be adjusted. In our study, we emphasized the significance of optimizing the hyperparameters for our Long Short-Term Memory (LSTM) network, which was employed for estimating room temperature in a setting of FDM printing. Variations in training and testing datasets distribution allowed us to adjust the LSTM network's design. Using a variety of data distributions, our method led to the decision to divide the data so that training would receive two-thirds of the total. A third was set aside for testing at the same time.

We looked at several choices for choosing optimizers for the LSTM network. Due to the Adam optimizer's success in enhancing intricate neural network topologies, we decided it after careful consideration. Several tests involving various optimizer candidates formed the basis for the choice. To establish the ideal learning rate for training the LSTM network, we ran tests utilizing a range of learning rate values. We arrived at a learning rate of 0.001 after extensive study, indicating optimal convergence and performance throughout training.

We also investigated how to set up batch sizes and the number of epochs needed to train the LSTM model with sequential data. After a thorough analysis, we determined that a batch size of 32 and 1000 epochs produced the greatest outcomes in terms of model generalization and optimization. Hyperparameters that were adjusted and listed in Table 2 included the structure and configuration of the LSTM network. Specifically, the network consisted of one input layer, one hidden layer, and one output layer. To receive the input data and prepare it for further processing, the input layer was essential. The LSTM network's input layer received a three-dimensional array as input. Different elements of the incoming data were represented by dimensions of this array. The batch size, which controls how many samples are processed during each training cycle, was represented by the first dimension. The second dimension was the time step, which represents the length of the sequence, or the number of prior time steps considered for prediction. The third dimension, which referred to the features or variables included in the input data, represented the quantity of units in the input sequence.

Table 2: LSTM model parameters setting

| Hyperparameters	Value
Train to total data ratio	66.67%
Test to total data ratio	33.33%
Optimizer	ADAM
Learning rate	0.001
Batch size	32
Number of epochs	1000
Amount of test data prediction	498
Amount of total data	1494

The input layer was able to manage and analyze the time series dataset efficiently by employing a three-dimensional array as input. To accurately anticipate room temperature for the FDM printing process, the network must be able to recognize the temporal correlations and patterns inherent in the data. Eight LSTM cells in hidden layer were also set up in the developed LSTM network. The capacity of the network to learn and represent complicated relationships in the data depends on the number of LSTM cells in the hidden layer.

To assess the pattern learning capability of our LSTM network, we examined the validation loss and root mean square error (RMSE) metrics. These measures shed light on the efficacy and precision of our algorithm in predicting room temperature under various circumstances. After investigation, we noticed that our LSTM model's validation loss was 0.0019. The difference between the predicted values and the actual values of the validation dataset is represented by the validation loss. Our LSTM network has successfully learned the patterns and correlations in the room temperature time series data because there was a decreased validation loss, which denotes a better fit of the model to the data.
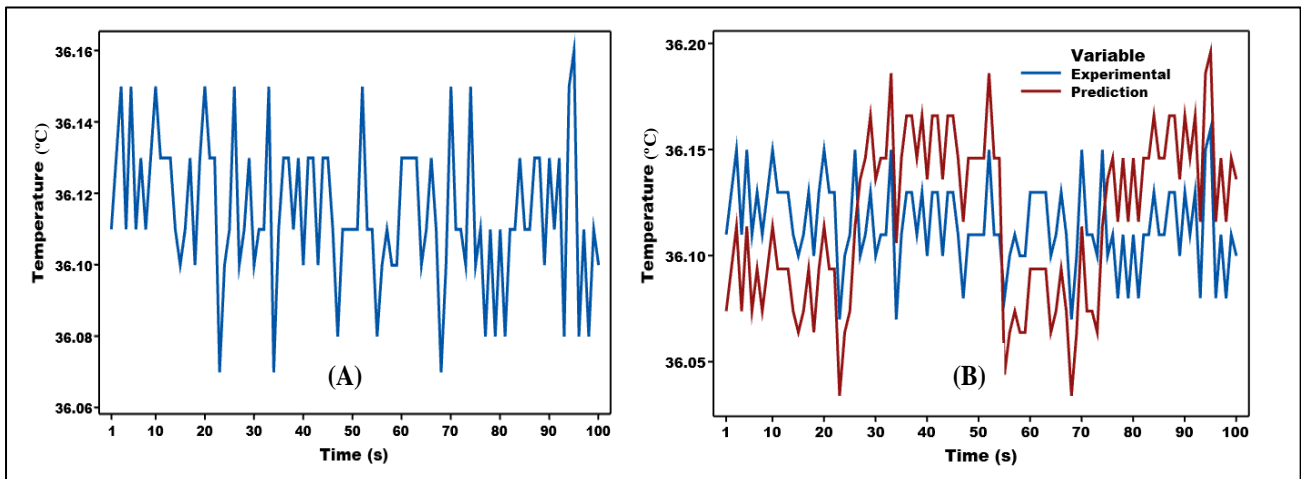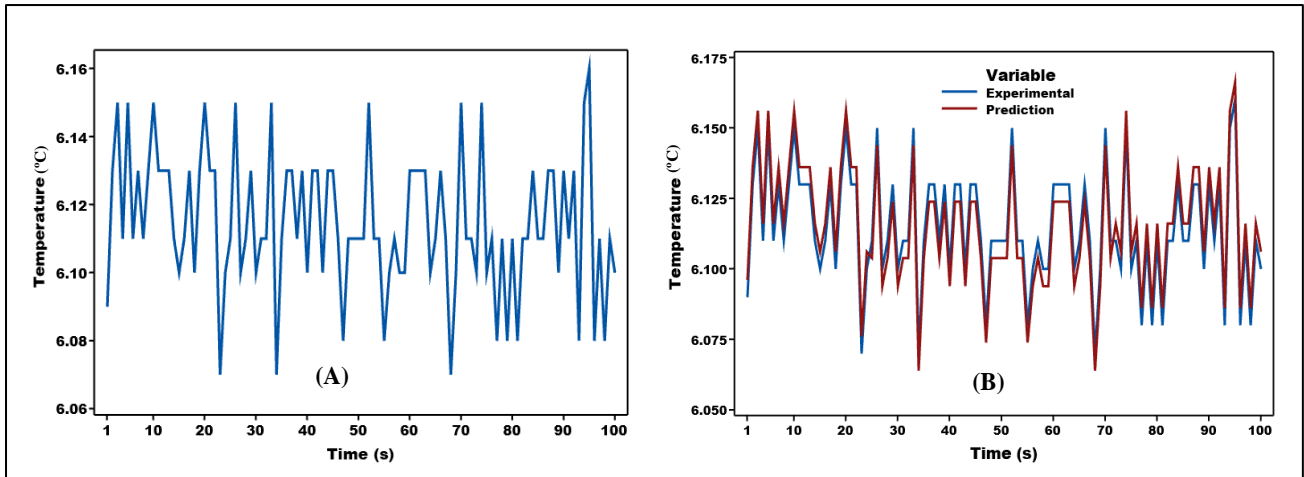

Fig 7: First 100 training datasets (A) with its prediction (B) at hot temperatures
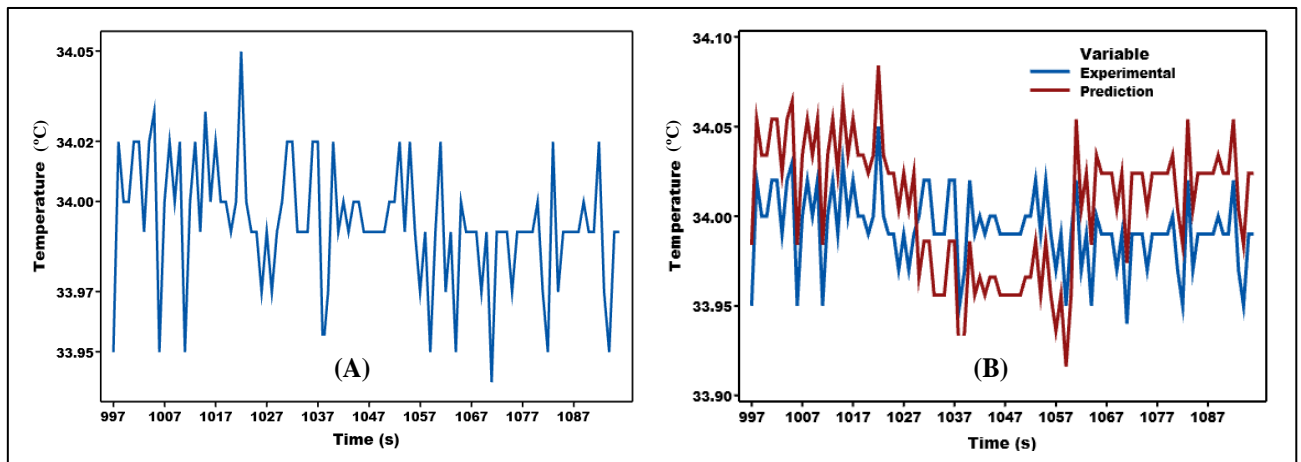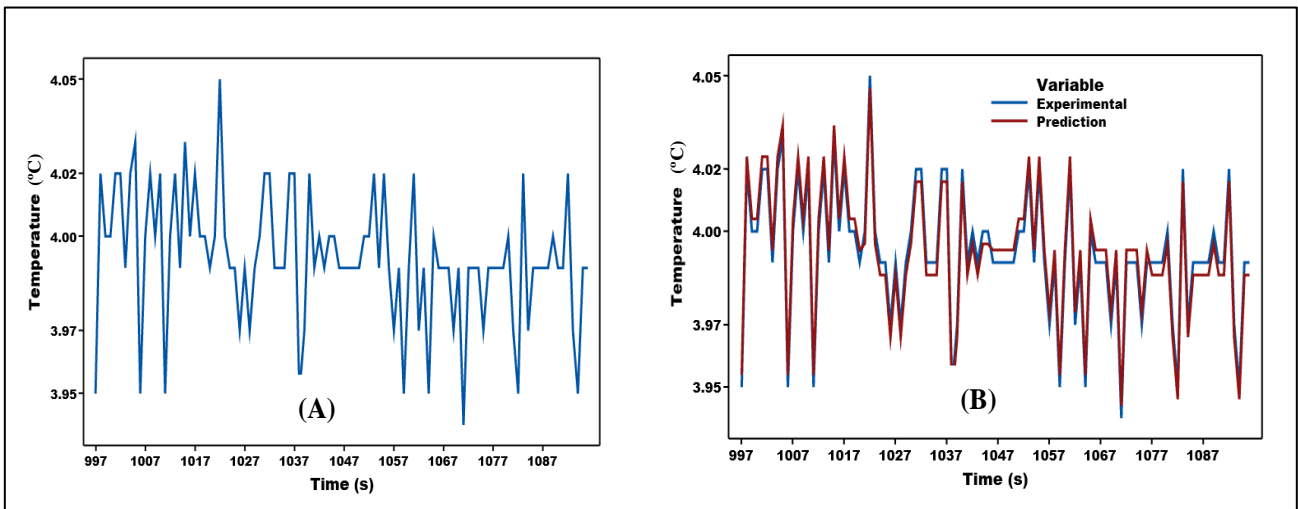

Fig 8: First 100 testing datasets (A) with its prediction (B) at hot temperatures

The accuracy of the model is demonstrated by the RMSE, which calculates the average discrepancy between the predicted values and the actual values. The RMSE was determined to be 0.033993 for the data points from the testing for severe temperatures. This number represents the typical discrepancy between expected and observed temperatures under extreme conditions. On the other hand, for the cold temperature testing data points, the RMSE was 0.003993, indicating a lower average error compared to the extreme temperature case. These findings suggest that our LSTM model was more precise in predicting room temperatures during cold temperature conditions compared to extreme temperature conditions. The lower RMSE for the cold temperature data points indicates that the model's predictions aligned closely with the actual temperature values, demonstrating its effectiveness in capturing the patterns and variations in cold temperature conditions.

Fig 9: First 100 training datasets (A) with its prediction (B) at cold temperatures

Fig 10: First 100 testing datasets (A) with its prediction (B) at cold temperatures

The measures, including the validation loss and root mean square error (RMSE), gave us important information about how well our LSTM model correctly predicted data for room temperature. These measurements demonstrated how well the algorithm was able to learn from the data and spot trends. Based on the outcomes of our research, we found that the LSTM model correctly predicted the data for room temperature, as shown in Figures 7-10. To illustrate the accuracy of the predictions, we specifically focused on the first 100 predicted data points from both the training and testing datasets. These subsets were chosen to provide a representative sample of the model's performance. Fig. 7 and 8 depict the predicted values for the first 100 extreme temperature data points from the training and testing datasets, respectively. By comparing the predicted values with the actual values, we can visually assess the accuracy of the model's predictions for extreme temperature conditions. Similarly, Figures 9 and 10 present the predicted values for the first 100 cold temperature data points from the training and testing datasets. These figures allow us to evaluate the accuracy of the model's predictions in capturing the patterns and variations in cold temperature conditions.

By examining these figures, we can observe how closely the predicted values align with the actual values. If the predicted values closely match the actual values, it indicates that the LSTM model successfully learned and captured the underlying patterns in the room temperature data. Overall, these visual representations of the predicted values provide a clear demonstration of the accuracy of our LSTM model in predicting room temperature. The close alignment between the predicted and actual values in Figs. 8-11 supports the effectiveness of the model in capturing and forecasting the temperature patterns, both in extreme temperature conditions and cold temperature conditions.

4.2 Effect of Temperatures on Product Quality

In our study, we observed that the quality of the printed parts was significantly impacted by the severe room temperatures. The heat from the built plate disappeared quickly when the room temperature was too low, causing a drop in temperature below the desired level. Due to this, some of the print pulled away during printing since the material did not cling to the build plate properly. As a result, our printed prototype had an upper surface that was rough, with a roughness measurement

of 4.001 μm. On the other hand, when the environment was too warm, the materials adhered to the build plate excessively due to the high temperatures. This made it challenging to remove the printed parts out of the build plate after they were produced. Our printed items have a surface roughness of 3.473 μm because of the high adherence. These results emphasize the need of preserving an ideal ambient temperature throughout the FDM printing procedure. The quality and adhesion of printed items can suffer under extreme temperatures.

In summary, the results of our investigation led to the following conclusions: the most accurate prediction on time series data for room temperature was made by the LSTM network, which had one input layer, one hidden layer with eight LSTM blocks, and one output layer. Our findings showed that the LSTM model was able to accurately reproduce the data on actual room temperature. As a result, it can be inferred that the model accurately depicted the patterns and trends in the temperature variations experienced during the FDM printing process. The ability to predict the room temperature accurately is useful because it gives information about the thermal conditions that can have an impact on the output quality of printed materials. By utilizing the developed LSTM network, an individual user could identify the quality of products during the printing process through surface roughness in the printed parts. The highest surface roughness was observed in measuring the prototype parts printed in cold room temperature environment than extreme room temperature.

5. CONCLUSION
In our study, we investigated the influence of time series room temperature data on the quality of products in FDM printing. To gain insights into this relationship, we developed a Long Short-Term Memory (LSTM) neural network model. This model was trained to forecast room temperature data based on the experimental time series data collected during the printing process. By training the LSTM model on the available room temperature data, we enabled it to learn the underlying patterns and relationships in the temperature fluctuations over time. To evaluate the accuracy of the LSTM model's predictions, we used the Root Mean Square Error (RMSE) metric. By understanding and predicting room temperature variations, manufacturers can take proactive measures to optimize the printing conditions and minimize the potential negative impacts on product quality. The LSTM model offers a data-driven approach to forecast room temperature, enabling users to make informed decisions and adjustments to ensure the desired printing outcomes. Future research should be focused on developing a time series room temperature prediction model based on various process parameter levels to provide the user more control in product quality prediction. Moreover, similar models can potentially be applied to time series room temperature data prediction in other additive manufacturing technologies.

REFERENCES
1. Prakash, K. S., Nancharaih, T., & Rao, V. S. (2018). Additive manufacturing techniques in manufacturing-an overview. *Materials Today: Proceedings*, *5*(2), 3873-3882.
2. Duty, C. E., Kunc, V., Compton, B., Post, B., Erdman, D., Smith, R., ... & Love, L. (2017). Structure and mechanical behavior of Big Area Additive Manufacturing (BAAM) materials. *Rapid Prototyping Journal*, *23*(1), 181-189.
3. Watson, J. K., & Taminger, K. M. B. (2018). A decision-support model for selecting additive manufacturing versus subtractive manufacturing based on energy consumption. *Journal of Cleaner Production*, *176*, 1316-1322.
4. Ahsan, N., & Khoda, B. (2016). AM optimization framework for part and process attributes through geometric analysis. *Additive Manufacturing*, *11*, 85-96.
5. Deb, J., Ahsan, N., & Majumder, S. (2022). Modeling the Interplay Between Process Parameters and Part Attributes in Additive Manufacturing Process With Artificial Neural Network. IMECE2022, Volume 2A: Advanced Manufacturing. https://doi.org/10.1115/IMECE2022-95120.
6. Liu, C., Xu, N., Zong, Q., Yu, J., & Zhang, P. (2021). Hydrogel prepared by 3D printing technology and its applications in the medical field. *Colloid and Interface Science Communications*, *44*, 100498.
7. Stavropoulos, P., & Foteinopoulos, P. (2018). Modelling of additive manufacturing processes: a review and classification. *Manufacturing Review*, *5*, 2.
8. Roney, M. D. S. R., Ahsan, N., Sezer, H., Tang, J., Kaul, S., & Ahmed, H. (2022). Modeling Thermal Behavior and Residual Stress for Layer-by-Layer Rotated Scan Direction in Laser Powder Bed Fusion Process. IMECE2022, Volume 2A: Advanced Manufacturing. https://doi.org/10.1115/IMECE2022-95355.
9. Moradi, M., Aminzadeh, A., Rahmatabadi, D., & Hakimi, A. (2021). Experimental investigation on mechanical characterization of 3D printed PLA produced by fused deposition modeling (FDM). *Materials Research Express*, *8*(3), 035304.
10. Jin, Z., Zhang, Z., & Gu, G. X. (2019). Autonomous in-situ correction of fused deposition modeling printers using computer vision and deep learning. *Manufacturing Letters*, *22*, 11-15.
11. Charalampous, P., Kostavelis, I., Kontodina, T., & Tzovaras, D. (2021). Learning-based error modeling in FDM 3D printing process. *Rapid Prototyping Journal*, *27*(3), 507-517.
12. Agron, D. J. S., Lee, J. M., & Kim, D. S. (2021). Nozzle Thermal Estimation on Fusion Deposition

Modeling Technique in Additive Manufacturing using Shallow Recurrent Neural Network. 한국통신학회 학술대회논문집, 495-496.

13. Pulipaka, A., Gide, K. M., Beheshti, A., & Bagheri, Z. S. (2023). Effect of 3D printing process parameters on surface and mechanical properties of FFF-printed PEEK. *Journal of Manufacturing Processes*, 85, 368-386.

14. Kim, H., Lin, Y., & Tseng, T. L. B. (2018). A review on quality control in additive manufacturing. *Rapid Prototyping Journal*, 24(3), 645-669.

15. Wong, K. V., & Hernandez, A. (2012). A review of additive manufacturing. *International scholarly research notices*, 2012(1), 208760.

16. Wang, P., Yang, Y., & Moghaddam, N. S. (2022). Process modeling in laser powder bed fusion towards defect detection and quality control via machine learning: The state-of-the-art and research challenges. *Journal of Manufacturing Processes*, 73, 961-984.

17. Alam, M. S. (2021). *An intelligent system approach for predicting air traffic demand based on socio-economic parameters*. The University of Regina (Canada).

18. Deb, J. B., Chowdhury, S., & Ali, N. M. (2024). An investigation of the ensemble machine learning techniques for predicting mechanical properties of printed parts in additive manufacturing. *Decision Analytics Journal*, 100492. https://doi.org/10.1016/j.dajour.2024.100492.

19. Deb, J. B., Gou, J., Song, H., & Maiti, C. (2024). Machine learning approaches for predicting the ablation performance of ceramic matrix composites. *Journal of Composites Science*, 8(3), 96.

20. Alam, M. S., Deb, J. B., Al Amin, A., & Chowdhury, S. (2024). An artificial neural network for predicting air traffic demand based on socio-economic parameters. *Decision Analytics Journal*, 10, 100382. https://doi.org/10.1016/j.dajour.2023.100382.

21. Westphal, E., & Seitz, H. (2021). A machine learning method for defect detection and visualization in selective laser sintering based on convolutional neural networks. *Additive Manufacturing*, 41, 101965.

22. Hussain, M. D., Rahman, M. H., & Ali, N. M. (2024). Investigation of Gauss-Seidel Method for Load Flow Analysis in Smart Grids. *Sch J Eng Tech*, 5, 169-178.

23. Hussain, M. D., Rahman, M. H., & Ali, N. M. (2024). Artificial Intelligence and Machine Learning Enhance Robot Decision-Making Adaptability and Learning Capabilities Across Various Domains. *International Journal of Science and Engineering*, 1(3), 14-27.

24. Kim, H., Lee, H., Kim, J. S., & Ahn, S. H. (2020). Image-based failure detection for material extrusion process using a convolutional neural network. *The International Journal of Advanced Manufacturing Technology*, 111(5), 1291-1302.

25. Qi, X., Chen, G., Li, Y., Cheng, X., & Li, C. (2019). Applying neural-network-based machine learning to additive manufacturing: current applications, challenges, and future perspectives. *Engineering*, 5(4), 721-729.

26. Liu, C., Law, A. C. C., Roberson, D., & Kong, Z. J. (2019). Image analysis-based closed loop quality control for additive manufacturing with fused filament fabrication. *Journal of Manufacturing Systems*, 51, 75-86.

27. Hu, H., He, K., Zhong, T., & Hong, Y. (2020). Fault diagnosis of FDM process based on support vector machine (SVM). *Rapid Prototyping Journal*, 26(2), 330-348.

28. Khan, M. F., Alam, A., Siddiqui, M. A., Alam, M. S., Rafat, Y., Salik, N., & Al-Saidan, I. (2021). Real-time defect detection in 3D printing using machine learning. *Materials Today: Proceedings*, 42, 521-528.

29. Banadaki, Y., Razaviarab, N., Fekrmandi, H., & Sharifi, S. (2020). Toward enabling a reliable quality monitoring system for additive manufacturing process using deep convolutional neural networks. *arXiv preprint arXiv:2003.08749*.

30. Wu, H., Yu, Z., & Wang, Y. (2017). Real-time FDM machine condition monitoring and diagnosis based on acoustic emission and hidden semi-Markov model. *The International Journal of Advanced Manufacturing Technology*, 90, 2027-2036.

31. Wu, H., Wang, Y., & Yu, Z. (2016). In situ monitoring of FDM machine condition via acoustic emission. *The International Journal of Advanced Manufacturing Technology*, 84, 1483-1495.

32. Equbal, A., Akhter, S., Equbal, M. A., & Sood, A. K. (2021). Application of machine learning in fused deposition modeling: a review. *Fused Deposition Modeling Based 3D Printing*, 445-463.

33. Kim, J. S., Lee, C. S., Kim, S. M., & Lee, S. W. (2018). Development of data-driven in-situ monitoring and diagnosis system of fused deposition modeling (FDM) process based on support vector machine algorithm. *International Journal of Precision Engineering and Manufacturing-Green Technology*, 5, 479-486. https://doi.org/10.1007/s40684-018-0051-4.

34. Paraskevoudis, K., Karayannis, P., & Koumoulos, E. P. (2020). Real-time 3D printing remote defect detection (stringing) with computer vision and artificial intelligence. *Processes*, 8(11), 1464.

35. Islam, M. S. (2021). A Data-Driven Approach using Long-Short Term Memory for Fault Prognosis and Remaining Useful Life Estimation of Satellite Reaction Wheel.

36. Islam, M. S., & Rahimi, A. (2020, October). Use of a data-driven approach for time series prediction in fault prognosis of satellite reaction wheel. In *2020 IEEE International Conference on Systems, Man, and Cybernetics (SMC)* (pp. 3624-3628). IEEE.

37. Islam, M. S., & Rahimi, A. (2021). A three-stage data-driven approach for determining reaction wheels' remaining useful life using long short-term memory. *Electronics*, *10*(19), 2432.

38. Islam, M. S., & Rahimi, A. (2021, June). Fault prognosis of satellite reaction wheels using a two-step LSTM network. In *2021 IEEE International Conference on Prognostics and Health Management (ICPHM)* (pp. 1-7). IEEE. https://doi.org/10.1109/ICPHM51084.2021.9486655.

39. Zhao, Y., Zhang, Y., & Wang, W. (2021, August). Research on condition monitoring of FDM equipment based on LSTM. In *2021 IEEE International Conference on Advances in Electrical Engineering and Computer Applications (AEECA)* (pp. 612-615). IEEE.

40. Saniman, M. N. F., Hashim, M. M., Mohammad, K. A., Abd Wahid, K. A., Muhamad, W. W., & Mohamed, N. N. (2020). Tensile characteristics of low density infill patterns for mass reduction of 3D printed polylactic parts. *International Journal of Automotive and Mechanical Engineering*, *17*(2), 7927-7934.

41. Kumar, N., Jain, P. K., Tandon, P., & Pandey, P. M. (2018). The effect of process parameters on tensile behavior of 3D printed flexible parts of ethylene vinyl acetate (EVA). *Journal of Manufacturing Processes*, *35*, 317-326.

42. Hikmat, M., Rostam, S., & Ahmed, Y. M. (2021). Investigation of tensile property-based Taguchi method of PLA parts fabricated by FDM 3D printing technology. *Results in Engineering*, *11*, 100264.

43. Hu, Y., Huber, A., Anumula, J., & Liu, S. C. (2018). Overcoming the vanishing gradient problem in plain recurrent networks. *arXiv preprint arXiv:1801.06105*.

44. Hochreiter, S., & Schmidhuber, J. (1997). Long short-term memory. *Neural Computation*, 9, 1735–1780.

45. Zhang, J., Zeng, Y., & Starly, B. (2021). Recurrent neural networks with long term temporal dependencies in machine tool wear diagnosis and prognosis. *SN Applied Sciences*, *3*(4), 442.

46. Sherstinsky, A. (2018). Fundamentals of Recurrent Neural Network (RNN) and Long Short-Term Memory (LSTM) Network. eprint. arXiv Preprint arXiv:180803314.

47. Deb, J. B. (2023). Data-Driven Prediction Modeling for Part Attributes and Process Monitoring in Additive Manufacturing. M.S. Western Carolina University.

48. Deb, J. B., Chowdhury, S., Chowdhury, S., Paul, G., Pal, T., Deb, J., & Deb, S. (2024). Machine acceleration time series prediction for dimensional accuracy of 3D printed parts. *Data Science and Management*. https://doi.org/10.1016/j.dsm.2024.02.002.